Climate Dynamics
https://doi.org/10.1007/s00382-020-05392-2

Projected changes in vertical temperature profiles for Australasia

Fei Ji[1] · Jason P. Evans[2] · Giovanni Di Virgilio[2] · Nidhi Nishant[1] · Alejandro Di Luca[2] · Nicholas Herold[1] · Stephanie M. Downes[1] · Eugene Tam[1] · Kathleen Beyer[1]

Received: 3 February 2020 / Accepted: 22 July 2020

Abstract
The vertical temperature profile in the atmosphere reflects a balance between radiative and convective processes and interactions with the oceanic and land surfaces. Changes in vertical temperature profiles can affect atmospheric stability, which in turn can impact various aspects of weather systems. In this study, we analyzed recent-past trends of temperature over the Australian region using a homogenized monthly upper-air temperature dataset and four reanalysis datasets (NCEP, ERA-Interim, JRA-55 and MERRA). We also used outputs of 12 historical and future regional climate model (RCM) simulations from the NSW/ACT (New South Wales/Australian Capital Territory) Regional Climate Modelling (NARCliM) project and 6 RCM simulations from the CORDEX (Coordinated Regional Downscaling Experiment) Australasian project to investigate projected changes in vertical temperature profiles. The results show that the currently observed positive trend in the troposphere and negative trend in the lower stratosphere will continue in the future with significant warming over the whole troposphere and largest over the middle to upper troposphere. The increasing temperatures are found to be latitude-dependent with clear seasonal variations, and a strong diurnal variation for the near surface layers and upper levels in tropical regions. Changes in the diurnal variability indicate that near surface layers will be less stable in the afternoon leading to conditions favoring convective systems and more stable in the early morning which is favorable for temperature inversions. The largest differences of future changes in temperature between the simulations are associated with the driving GCMs, suggesting that large-scale circulation plays a dominant role in regional atmospheric temperature change.

Keywords Temperature trend · NARCliM · Ensemble mean · Change in vertical temperature

1 Introduction

The vertical temperature profile reflects a balance between radiation, and convective and dynamical heating/cooling of the coupled surface-atmospheric system. Vertical temperature profiles are widely used in weather forecasting and climate modelling. For example, vertical temperature profiles are used to calculate convective available potential energy (CAPE) for convective weather system forecasts (Ziarani et al. 2019). Vertical temperature profiles are also used to identify temperature inversions (Bourne et al. 2010; Ji et al. 2018), which can be used for air quality forecasting.

Any changes in a vertical temperature profile will influence atmospheric stability, and this will directly impact different weather systems (Raju et al. 2014; Zheng et al. 2015; Stovern and Ritchie 2016; Ma et al. 2017). Raju et al. (2014) assessed the impact of vertical temperature profile changes on the Asian Summer monsoon. Their study suggested that the assimilation of vertical temperature profiles in regional climate models can significantly improve the dynamical and thermodynamical features of monsoon simulation by representing the vertical distribution of temperature more realistically. Several studies have demonstrated the importance of vertical temperature structure on the development of tropical cyclones (Zheng et al. 2015; Stovern and Ritchie 2016; Ma et al. 2017).

Electronic supplementary material The online version of this article (https://doi.org/10.1007/s00382-020-05392-2) contains supplementary material, which is available to authorized users.

✉ Fei Ji
fei.ji@environment.nsw.gov.au

[1] Science, Economics and Insights, NSW Department of Planning, Industry and Environment, Sydney, Australia

[2] Climate Change Research Centre and ARC Centre of Excellence for Climate Extremes, University of New South Wales, Sydney, Australia

Published online: 30 July 2020

Vertical temperature profiles are critical to weather forecasts and climate studies, however, there are only 1300 in-situ monitoring sites globally (https://www.wmo.int/pages/prog/www/OSY/Gos-components.html), in which vertical temperature profiles are collected via radio sounding. There has been much effort to retrieve vertical temperature profiles from different passive and active remote sensors such as GPS radio occultation (Zhang et al. 2011), Light Detection and Ranging (LIDAR) (Newsom et al. 2013), infrared and microwave (Blumberg et al. 2015), microwave (Aires et al. 2015) and infrared sounder (Zhang et al. 2016). Several studies have compared retrieved vertical temperature profiles to local, regional or global raw/homogenized radiosonde data (Christy and Norris 2006, 2009; Christy et al. 2007, 2009, 2011; Randall and Herman 2008; Mears et al. 2012; Po-Chedley and Fu 2012). These satellite data have contributed to the improvement of weather forecast accuracy (Chahine et al. 2006; Chikira and Sugiyama 2010; Jones and Stensrud 2012).

Several studies have analysed long-term vertical temperature profiles collected from traditional and satellite retrieved soundings (Aikawa and Hiraki 2009; Pralungo and Haimberger 2015; Jovanovic et al. 2017). Aikawa and Hiraki (2009) collected 5 years of temperature data at different vertical levels in Japan to analyse the seasonality of vertical air temperature profiles in an urban coastal area. Their results showed characteristic seasonality in the vertical air temperature profile. Hartmann et al. (2013) assessed multiple independent analyses of measurements from radiosondes and satellite sensors and concluded that the troposphere has warmed globally whereas the stratosphere has cooled since the mid-twentieth century. Pralungo and Haimberger (2015) used historical radiosonde and pilot balloon wind shear observations with the aim to reduce uncertainties in the estimation of strong trend amplification in the tropical upper troposphere. Their best estimates for the warming maxima in the upper tropical troposphere agreed well with those directly from observed temperatures but tended to be located at higher altitudes. Jovanovic et al. (2016) developed a homogenized monthly upper-air temperature dataset for 22 stations across Australia and 5 Australian remote island sites for 1958–2011. Their analysis of the linear trend in temperature for each level showed significant changes in temperature, i.e. a general warming in the troposphere, a cooling in the lower stratosphere and a faster warming in the troposphere as compared to the surface level.

Several model-based studies have attempted to explain observed temperature changes in the troposphere and lower stratosphere. Most of these studies have reported faster warming of the troposphere than the surface, and cooling of the lower stratosphere (Ramaswamy et al. 2006; Hartmann et al. 2013). Santer et al. (2006) used multiple global climate models (GCMs) to simulate observed changes in vertical temperature profiles and investigated possible causes of recent temperature changes both at the Earth's surface and in the free atmosphere. They showed that both natural and anthropogenic factors contributed to changes in the vertical temperature. Despite recent advances in analysing atmospheric vertical temperature profiles, there is still a lot to learn in possible future changes in vertical temperature profiles.

Multiple studies have already shown that dynamical downscaling can provide added value to the simulation of some natural phenomena, as compared to driving GCMs (Di Luca et al. 2013, 2016b; Di Virgilio et al. 2020). Regional climate model (RCM) simulations provide not only finer spatial and temporal modelling outputs to suit local/regional impact assessments but also more accurate results. In this study, we use regional dynamical downscaling outputs from the NARCliM (New South Wales/Australian Capital Territory Regional Climate Modelling) project (Evans et al. 2014) and data from the CORDEX (Coordinated Regional Downscaling Experiment) project to investigate how the vertical temperature profiles are projected to change in the future for the Australasia region. We quantify the mean changes in temperature at different atmospheric levels in the troposphere and lower stratosphere. We also quantify seasonal and diurnal variations of changes in the temperature profile. Before investigating future changes in vertical temperature simulated by dynamical downscaling, we also investigate the changes in vertical temperature in observation and reanalysis datasets. Temperature trends found in the observations are then compared to projections of future changes in temperature.

2 Methods

2.1 Data

2.1.1 Monitoring data

Homogenized monthly upper-air temperature for 22 stations across the Australian Continent and one Australian remote island site are produced by the Australian Bureau of Meteorology (Jovanovic et al. 2016). The data quality control process involved the examination of station metadata and an objective statistical test to detect discontinuities in the data. Four out of the 23 stations are located between 10 and 20° S, and 9 stations are located between both 20° S and 30° S, and 30° S and 40° S. There is only one station which is south of 40° S. The large spread of the stations allows us to analyse observed changes for different latitudes. The details of each station (station number, station name, latitude and longitude, and start year) are described in Table S1.

The monitoring data is based on 2300 UTC (local time 9 a.m. AEST) radiosonde soundings with most records starting in 1958. Mean surface temperature from the Australian Climate Observations Reference Network—Surface Air Temperature (ACORN-SAT) (Trewin 2013) is also included in the analysis. In total, this data set has 9 vertical levels (surface, 850, 700, 500, 400, 300, 200,150 and 100 hPa).

2.1.2 Reanalysis data

The four reanalysis data sets used in this study are National Centres for Environment Prediction (NCEP) (Kalnay et al. 1996), ECMWF Re-Analysis (ERA) Interim (Dee et al. 2011), the Japanese 55-year Reanalysis (JRA-55) (Kobayashi et al. 2015) and Modern-Era Retrospective Analysis for Research and Applications (MERRA) (Rienecker et al. 2011). NCEP data is produced by the National Centres for Environment Prediction in the United States. This data is available at 17 pressure levels from 1000 to 10hpa with a spatial resolution of 2.5°, from 1948 to present and is recorded four times a day. ERA-Interim is a global atmospheric reanalysis produced by the European Centre for Medium-Range Weather Forecasts (ECMWF) from 1979 to 2018. The spatial resolution of ERA-Interim is approximately 80 km (T255 spectral) with 60 vertical levels from the surface up to 0.1 hPa. The JRA-55 reanalysis was produced by the Japan Meteorological Agency, which is a 55-year global atmospheric reanalysis starting from 1958. The spatial resolution of the data set is roughly 55 km with 60 vertical levels from the surface up to 0.1 hPa. MERRA was undertaken by NASA's Global Modelling and Assimilation Office which is available from 1979 to the present. The spatial resolution of this data set is approximately 55 km ($1/2^{o} \times 2/3°$) with 72 vertical levels from the surface to 0.01 hPa.

2.1.3 Model data

2.1.3.1 NARCliM simulations The NARCliM project was developed to provide robust finer-scale climate projections for southeast Australia (Evans et al. 2014). Four GCMs were selected from the Coupled Model Intercomparison Project (CMIP3) GCMs ensemble to force three selected RCMs to form 12 GCM/RCM ensemble members. The four GCMs (MIROC3.2, ECHAM5, CCCMA3.1, and CSIRO-MK3.0) were selected based on GCMs' performance over Australia, independence of their errors, and to span the full range of potential future climates over south-eastern Australia (Evans et al. 2014). The three RCM configurations (R1, R2 and R3) are three physics scheme combinations of the Weather Research and Forecasting (WRF) V3.3 model (Skamarock et al. 2008). These were selected from a large set of 36 different combinations of physics parametrizations tested over eight significant East Coast Lows (Evans et al. 2012; Ji et al. 2014) and chosen based on model performance and independence of model errors (Evans et al. 2014). Each GCM/RCM member was run for 1990–2009 (historical period), 2020–2039 (near future) and 2060–2079 (far future) for two nested domains (Fig. 1). The outer domain is the CORDEX Australasia domain and the outputs from this domain were used in this study. NARCliM modelling is performed using a rotated pole map projection, output data are interpolated onto regular latitude/longitude grids from (50^{o} S, 110^{o} E) to (0^{o} S, 180^{o} E) using an inverse distance squared approach.

A number of studies have reported that the resultant ensemble from the NARCliM 12 GCM/RCM simulations improves substantially on the GCMs in the simulation of Australian mean and extreme climate (Olson et al. 2016; Evans et al. 2017). Using model independence makes it possible to develop relatively small ensembles that can reproduce the ensemble mean and variance from the large parent GCM ensemble as well as minimize the overall error (Evans et al. 2013a, b).

Evaluations of NARCliM simulations demonstrate that RCMs can simulate precipitation and surface temperature reasonably well (Ji et al. 2016), however, no individual RCM performs well for all variables, seasons and metrics compared to available observations. The use of the full NARCliM ensemble provides a measure of robustness such that any result that is common to all RCMs in the ensemble is considered to have higher confidence. Therefore, the multi-model mean is used to demonstrate the results for this study. As shown in Olson et al. (2016), changes in the near future relative to the historical period are relatively small, thus we focus our analyses on changes in temperature profiles in the far future (2060–2079).

Some studies have already shown that NARCliM can provide added value to the simulation of surface variables such as precipitation, maximum and minimum temperatures,

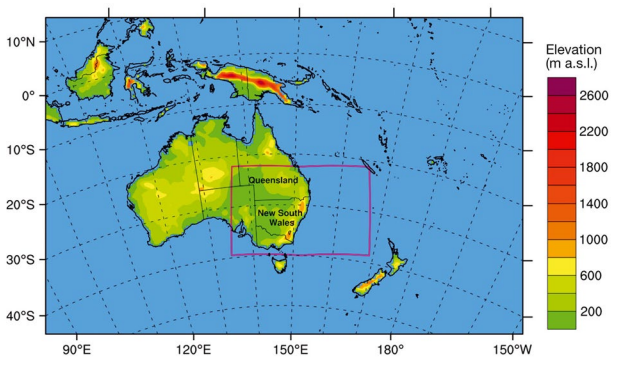

Fig. 1 Weather Research and Forecasting (WRF) model domains with grid spacing of about 50 km (outer CORDEX domain shown as map extent) and 10 km (inner NARCliM domain shown with red outline)

when compared to driving GCMs (Di Luca et al. 2013, 2016a, b; Di Virgilio et al. 2019a). Additional NARCliM evaluations include its representation of large-scale climate mode teleconnections (Fita et al. 2016), sub-daily rainfall extremes (Cortés-Hernández et al. 2015), extra-tropical low pressure systems (Di Luca et al. 2016a), fire-weather (Clarke and Evans 2019 and Di Virgilio et al. 2019a) and near surface winds (Evans et al. 2018) amongst others. In each case the ensemble was found to perform well overall, though errors were also noted. Ji et al. (2018) have shown that NARCliM simulations can capture temperature inversions reasonably well. This gives us confidence in using NARCliM outputs to assess future changes in vertical temperature.

2.1.3.2 CORDEX simulations CORDEX is an initiative of the World Climate Research Programme (WCRP) that aims to improve both the generation and evaluation of downscaled regional climate information (Giorgi et al. 2009). Under the CORDEX framework, regional climate projections based on CMIP5 GCM projections have been produced for fourteen regions worldwide. CORDEX Australasia currently comprises three configurations of the WRF model, one configuration of the Conformal Cubic Atmospheric Model (CCAM) model and one configuration of the COSMO Climate Limited-area Model (CCLM). CORDEX Australasia simulations are run by dynamically downscaling CMIP5 GCMs following the Representative Concentration Pathway (RCP8.5) scenario (Table 1). For assessing the RCMs' capabilities to simulate observed regional climate, ERA-Interim driven hind-cast simulation were run from 1979 to 2013 and evaluated against observations. CORDEX RCMs used in the evaluation and their configurations are summarized in Di Virgilio et al. (2019b). Currently, 6 GCM-forced CCAM simulations and one GCM (ACCESS1.3) driven 3 WRF configurations are available for historical (1951–2005) and future (2006–2100) periods (Table 1), which are used in the study.

2.2 Analysis techniques

Following Jovanovic (2016), we analyse the linear trend of the annual temperature time series for the 23 stations at each of the 9 vertical levels including the surface (at 2 m altitude). Recent studies have found, and our data confirms, that vertical temperature changes show larger differences between latitudes than between longitudes (e.g. Jovanovic et al. 2016), which indicates that temperature and vertical temperature changes are latitude dependent. We sort 23 stations according to latitude and analyse the temperature trend vs latitude for all vertical levels.

The same approach of temperature averaged along longitude is applied to all datasets including reanalyses and modelling outputs. We analysed the linear trend of zonal temperature at each latitude on each pressure level.

As only 20-year time slices are available in the NARCliM simulations for historical and future periods, differences in the zonal temperature between 2060–2079 and 1990–2009 are calculated for each latitude on each vertical level. For analysis of differences between land and ocean, we separate grids over land and ocean when we average temperature along longitude.

CORDEX simulations only provide temperature time series on three atmospheric levels (200, 500 and 850 hPa) and the surface level. We thus split latitude into five latitudinal zones (0–10° S, 10–20° S, 20–30° S, 30–40° S and 40–50° S), and average zonal temperature time series for each of the five latitude groups to obtain mean temperature time series on four vertical levels (including the surface). The changes in averaged temperature are then calculated between 2060–2079 and 1990–2009 for the CORDEX simulations in order to make the comparison with those derived from the NARCliM simulations.

The statistical significance of changes in individual simulations of atmospheric temperature profiles was estimated with respect to the inter-annual variability using a Students t-test at the 5% significance level ($p < 0.05$), assuming equal variances for the past and future simulated time series. The use of t-tests assumes that annual mean values follow a normal distribution in past and future periods. We then present the results on significance according to three categories (Tebaldi et al. 2011): areas with significant agreement (stippled), areas with insignificant agreement (shown in color), and areas with significant disagreement (shown in grey). In areas with significant agreement, at least half of the models show a significant change and at least 80% of significant models agree on the direction of change. We consider these changes to be robust within the ensemble. In areas with insignificant agreement, less than half of the models show significant changes. These are areas where the ensemble is projecting change that is not larger than the internal climate variability. In areas with significant disagreement, at least half of the models show a significant change, but less than 80% of significant models agree on the direction of the change. In these areas we have low confidence in the projected changes.

3 Results

3.1 Observed temperature changes over Australia

The observed linear trend of the mean annual temperature time series at the nine atmospheric levels for 23 stations is shown in Fig. 2. A positive trend is seen for temperature in the troposphere (200 hPa and below) whereas a negative

Table 1 Specifications of the model data sets used in this study

Project Name	Ensemble name	Model	Resolution and domain	Input models	Emissions scenario and periods used
NARCliM	New South Wales and Australian Capital Territory regional climate modelling (NARCLIM) project (Evans et al. 2014)	Weather Research and Forecasting (WRF)	50 km, CORDEX Australasia	4 CMIP3 Global Climate Models: 1. CCCMA CGCM3.1-t47 (run 4) 2. CSIRO-Mk3.0 (run 1) 3. MPI-OM-ECHAM5 (run 1) 4. MIROC3.2-medres (run 1) Three different WRF configurations (12 total simulations)	SRES A2 Time-slices 1990–2009, 2020–2039 and 2060–2079
CORDEX	**WRF-50**	Weather Research and Forecasting (WRF)	50 Km CORDEX Australasia	3 CMIP5 GCMs (all run 1): 1. ACCESS-1.0 2. ACCESS-1.3 3. CanESM2 Two different WRF configurations (6 total simulations)	RCP8.5 Continuous 1950–2100
	CCAM-50: Victorian projections for Department of Environment, Land, Water and Planning (DELWP) and Wine Australia (for methods see: McGregor et al. 2016)	Conformal Cubic Atmospheric Model (CCAM)	50 Km CORDEX Australasia	6 CMIP5 GCMs (all run 1): 1. ACCESS-1.0 2. CNRM-CM5 3. GFDL-ESM2M 4. HadGEM2-CC 5. MIROC5 6. NorESM1-M 1 CCAM configuration	RCP8.5 Continuous 1961–2100

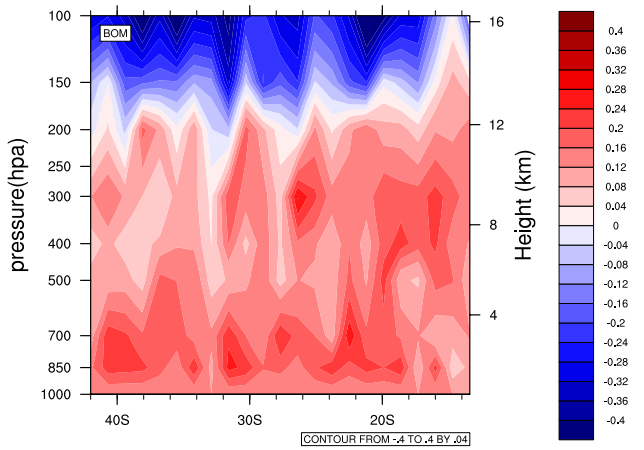

Fig. 2 Trend of vertical temperature for 1958–2011 for 23 Australian stations (unit: °C/decade) using the homogenized monthly upper-air and surface temperature data from Australian Bureau of Meteorology (BOM)

trend is seen for temperature in the lower stratosphere (approximately above180 hPa). The vertical variation of the trend in upper air temperature is similar to that of global observations for the Southern Hemisphere (Hartmann et al. 2013). In the Australasia region, temperature increases by approximately 0.3 and 0.2 °C per decade at 850 hPa and 300 hPa respectively. These results are partly consistent with global observation which shows a similar increase in temperature at 300 hPa over the Southern Hemisphere (Hartmann et al. 2013). All the trends in upper air temperature are found to be statistically significant at the 99.99% level, indicating an overall significant warming in the troposphere and a cooling in the lower stratosphere, as well as a comparatively faster warming of the troposphere than the surface.

3.2 Changes in global temperature profiles

Figure 3 shows the global linear trend of annual mean zonal temperature for the four reanalysis datasets (NCEP, ERA-I, JRA55 and MERRA). Overall, linear trends are similar between the four reanalysis datasets for the Northern Hemisphere. All the reanalysis data sets simulate cooling in the

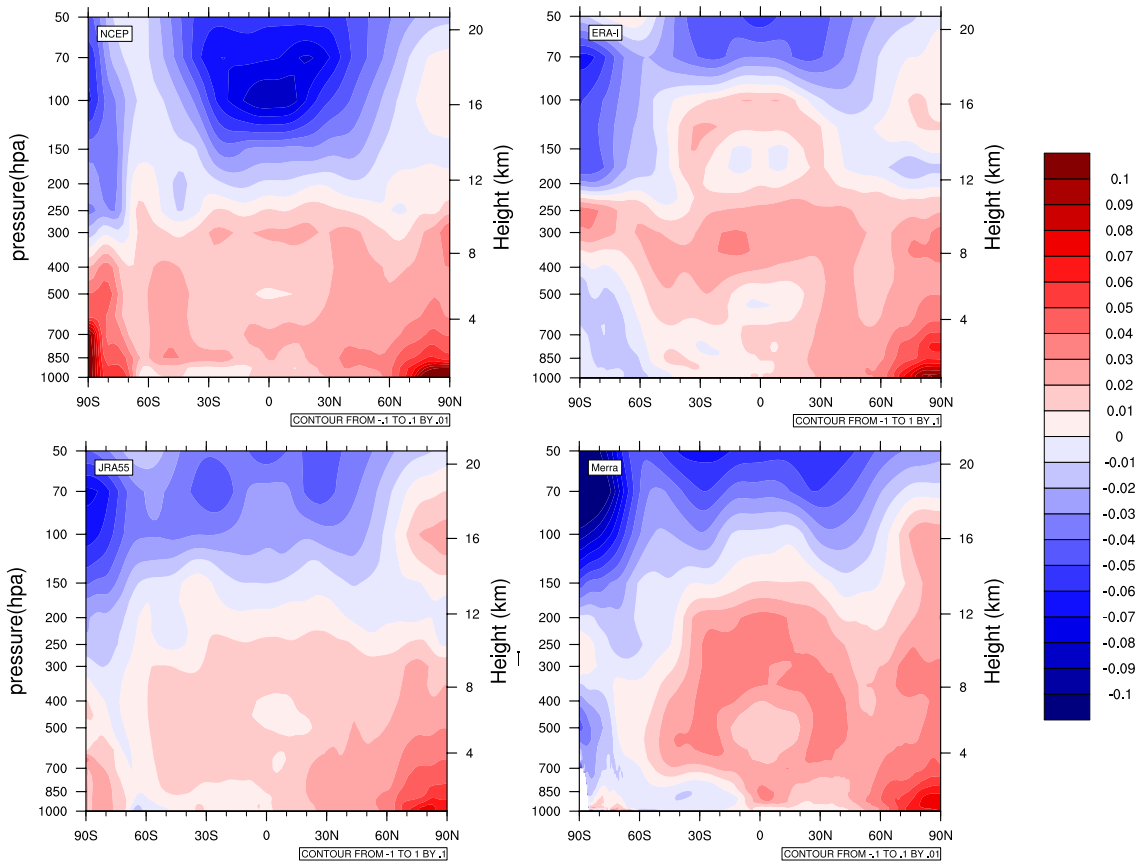

Fig. 3 Trend in annual mean temperature in the reanalysis data sets (NCEP, EAR-Interim, JRA55 and MERRA), unit (°C/decade). The temperature was averaged along longitude before it was used to calculate trend. Data from 1980 to 2014 are used for NCEP, ERA-Interim and MERRA, and 1977–2010 for JRA55

lower stratosphere (above 100 hPa) and warming in the troposphere (below 150 hPa). The atmosphere warms faster in the upper troposphere (300–400 hPa) in the tropical region. An extremely fast rate of warming in the North Pole region from the surface up through the troposphere is displayed by all reanalysis datasets, whereas the reverse applies to the South Pole region. A possible reason for the faster rate of warming in the North Pole can be attributed to the decline in extent of sea ice and snow due to global warming (Wang and Liang 2009).

Quite large differences can be observed between the four reanalyses, especially for the Southern Hemisphere, providing an indication of the observational uncertainty associated with these trends. However, all data sets simulated cooling in the lower stratosphere, warming in the upper and middle troposphere, and warming faster in upper levels than the surface, which is similar to patterns evident in the observed records (Fig. 2). It's worthy to note that temperature trend in reanalyses is generally smaller than that of observations.

3.3 Changes in future projections

3.3.1 Mean changes in Australasia temperature profiles

Multi-model mean of change in temperature profiles for 2060–2079 relative to 1990–2009 derived from the NARCliM simulations is shown in Fig. 4. The change in the temperature profiles is found to be latitude-dependent, especially for the middle and upper troposphere levels (i.e. between 500 and 150 hPa). A larger increase is simulated for the tropical region than for higher latitude regions, with more than a 4.6 °C increase for the 200–250 hPa layer in the tropical region and above 2.8 °C increase for the 300–400 hPa layer

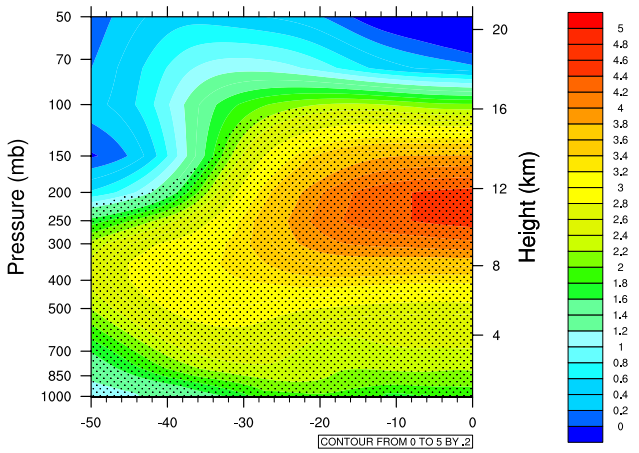

Fig. 4 Ensemble mean of changes in temperature derived from NARCliM ensemble: 2060–2079 minus 1990–2009. (unit: °C). Here the stripling denotes significant change and 80% agreement in the sign of the change between 12 ensemble members

in the temperate region. When compared with the trends in the observed (Fig. 2) and reanalysis data sets (Fig. 3), it is clear that warming will accelerate, and the altitude of maximum warming will increase in the future. In the lower troposphere, the change in temperature generally increases with height, but shows minor meridional variation. In contrast, the change in temperature generally decreases with height for the upper troposphere and lower stratosphere. When comparing the mean changes derived from the NARCliM simulations (Fig. 4) with their driving CMIP3 GCMs (Figure S1), it is shown that RCM simulations project larger warming in the troposphere and smaller cooling in the lower stratosphere than their driving GCMs, however their patterns of temperature changes are similar.

Given that CORDEX simulations only provide temperature on three atmospheric levels (200, 500 and 850 hPa) and the surface, it is not possible to show the vertical profile of changes in temperature for these data. We therefore compare the changes in zonal temperature between CORDEX and NARCliM for 2060–2079 relative to 1990–2009 for four levels, and the ensemble means are shown in Fig. 5. The CORDEX data clearly projects larger warming (0.2–1 °C for different latitude and levels) for the lower troposphere (500 hPa and below) as compared to NARCliM. This is understandable, because RCP8.5 in CMIP5 is more aggressive in terms of emissions than the A2 scenario in CMIP3. However, changes in temperature for CORDEX and NARCliM both show a similar variation in latitude for three levels (i.e. little variations between the equator to 20° S, and a general decrease from 30 to 50° S). Changes in temperature at 200 hPa are quite different from those for the lower troposphere, even though both are primarily latitude dependent. Much larger increases in temperature (1 ~ 2.1 °C for CORDEX and 1 ~ 1.8 °C for NARCliM) for the tropical region (0–20° S), and much smaller increase in temperature (− 2.9 ~ − 1.5 °C for CORDEX and − 1.6 ~ − 0.1 °C for NARCliM) for the sub-tropical and temperate region (30–50° S) were observed at 200 hPa, compared to those at 500 hPa. Furthermore, the changes in temperature at 200 hPa are even slower than those on the surface for high latitude (40–50° S). However, changes in temperature for CORDEX and NARCliM show similar variation in terms of latitude. Interestingly, changes for CORDEX are about 1 °C larger than those for NARCliM over the tropical region, but those for CORDEX are about 0.5 °C smaller than those for NARCliM over the sub-tropical and temperate regions (30–50° S).

The maximum warming in the tropical upper troposphere has been theoretically explained in Bony et al. (2006) as being associated with a decline in the moist adiabatic lapse rate of temperature in the tropics as the climate warms. The minimum warming in the upper troposphere at high latitudes is similar to those shown in Fig. 12.12 in the IPCC AR5

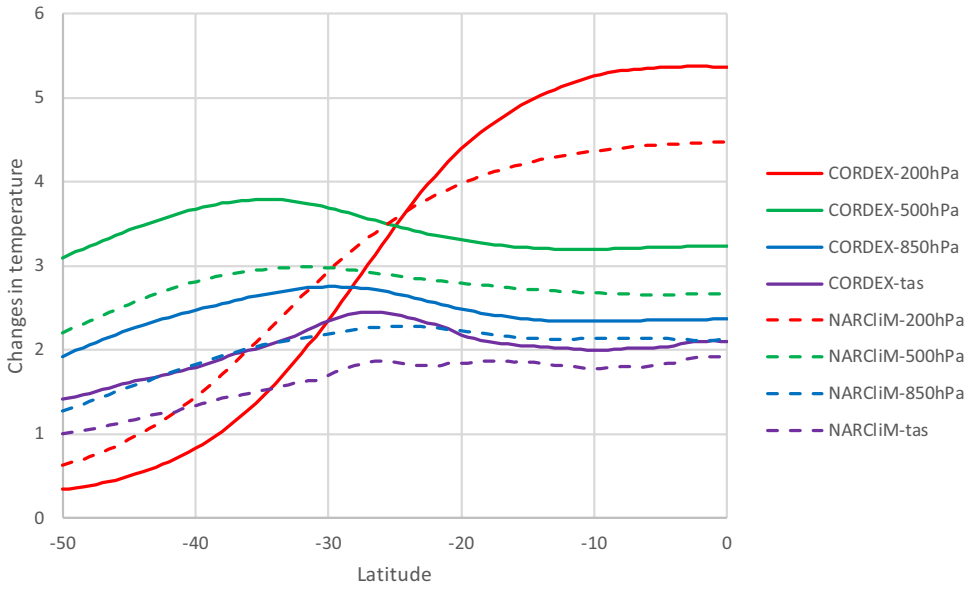

Fig. 5 Changes in temperature (2060–2079 minus 1990–2009) at four levels (200,500, 850 hPa and surface) for the NARCliM and CORDEX data sets (unit: °C). Solid and dash lines are for CORDEX and NARCliM respectively. Four different colours represent different levels

report (Collins et al. 2013) in which the higher emission scenario results in a smaller rate of temperature increase.

The atmospheric dynamics and the large-scale organization of the atmosphere is a strong function of latitude. In the tropics, large-scale overturning circulations prevail. Meanwhile, equatorial planetary waves enforce upwelling in tropics (Grise and Thompson 2012). These take more humidity to the upper levels through convections and result in the largest warming in tropical upper troposphere (Bony et al. 2006). In contrast, the low stratosphere becomes cooler due to the depletion of low stratospheric ozone and increases in well-mixed gases that is the major radiative factor in accounting for the cooling (Ramaswamy and Schwarzkopf 2002).

The tropopause separates the stratosphere from the troposphere. The altitude of the tropopause decreases with increases in latitude and has a clear seasonal variation, especially for high latitude. 200 hPa is always in the troposphere in the tropics, however, it is above tropopause in the cold season and under tropopause in the warm season at high latitude, so it is warming in the warm season and cooling in the cold season that results in very small annual warming at high latitude. However, it is constantly warming in the middle and low troposphere. This leads to the warming at 200 hPa being smaller than the middle (500 hpa) and low (850 hpa) troposphere for high latitude.

3.3.2 Seasonal variation of changes in temperature

Changes in temperature show clear seasonal variation, with opposing patterns evident in Summer and Winter (Fig. 6). The most striking feature is strong seasonal variability in subtropical and temperate regions, with more than a 2 °C difference in the temperature change in the upper troposphere and lower stratosphere, and more than 0.6 °C difference in the lower troposphere, between summer and winter. Generally, more than a 1 °C anomalous increase in temperature is simulated in the upper troposphere and lower stratosphere in summer in the temperate region, in contrast, there is more than a 1 °C anomalous decrease in temperature in Winter. Seasonal variation is relatively small for the tropical region when compared with the sub-tropical and temperate regions. Middle and lower troposphere (below 300 hPa) generally show slower warming (− 0.3 °C) during summer over the tropical region. In contrast, warming is about 0.3 °C faster during winter in the tropical region, which is opposite to variation at the same levels for the temperate region. The upper troposphere generally shows the same direction of variation with that at the same level for the sub-tropical and temperate regions.

Spring and autumn appear to be transition seasons between summer and winter. The pattern of temperature change during autumn is similar to that during summer, though the former shows a much slower warming rate. Spring is similar to winter, but the former has a slightly faster warming rate, especially for the temperate and sub-tropical regions.

For the temperate region, the large seasonal variation between 10 and 20 km above ground is possibly associated with the seasonal variation of tropopause height, which is generally higher in summer and lower in winter (Rieckh et al. 2014). During summer, when the tropopause is lifted higher, the upper troposphere warms even if the warming rate is smaller compared with middle troposphere. In winter, when the tropopause drops, 10 km is above the tropopause and the atmosphere in the lower stratosphere will get cooler (Ramaswamy et al. 2006).

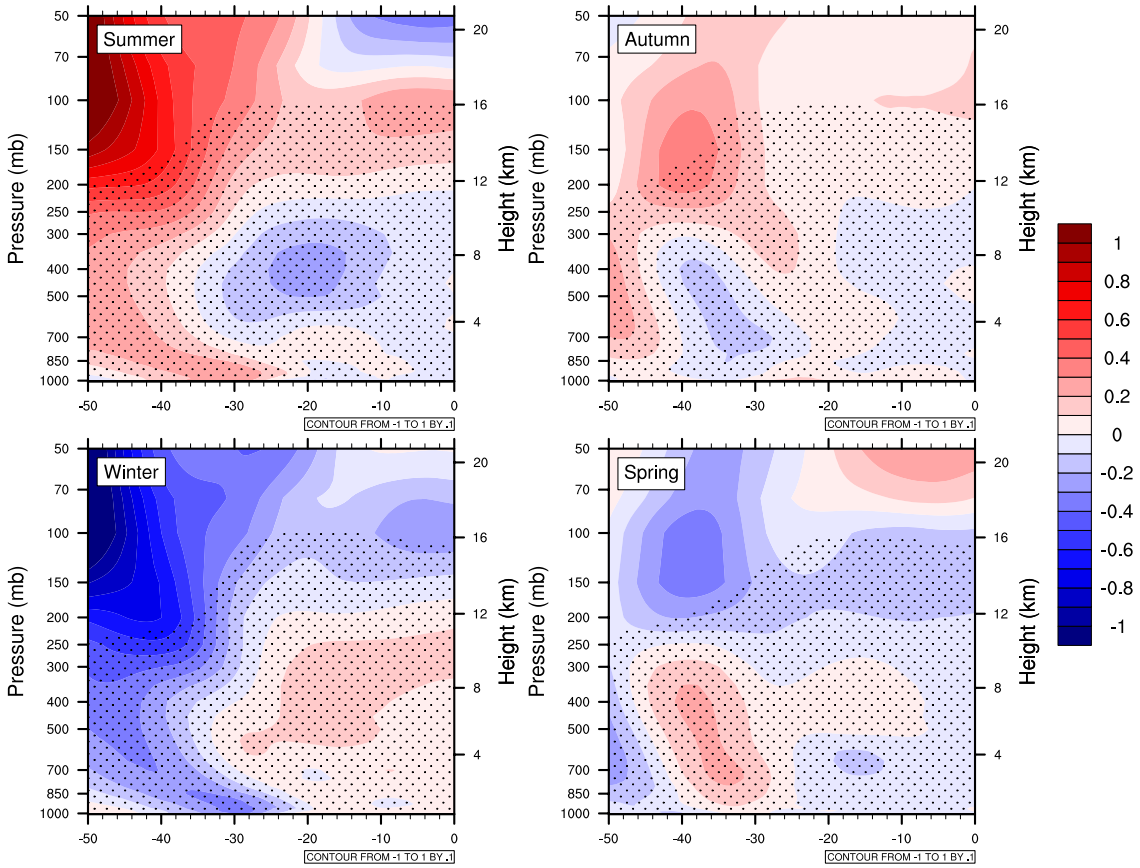

Fig. 6 Seasonal variation of anomaly (relative to annual change shown in Fig. 4) in temperature change (2060–2079 minus 1990–2009) for the NARCliM ensemble (unit: °C). Here the stripling denotes significant change and 80% agreement in the sign of the change between 12 ensemble members

3.3.3 Differences between land and ocean

Temperature changes show more than 0.3 °C difference between land and ocean at near surface levels (Fig. 7), which indicates that the atmosphere in near surface levels warms faster over land than over the ocean, especially in summer (Figure S3). This is consistent with a previous study by Byrne and O'Gorman (2013) that indicated surface temperatures increase at a greater rate over land than over ocean in simulations and observations of global warming. Other notable differences can be observed in the middle and upper troposphere in the sub-tropical region, where the atmosphere warms at a faster rate for the upper troposphere, and at a slower rate for the middle troposphere layers when comparing land and ocean. These differences could be caused by differences in cloud cover and cloud types. The bottom of clouds is generally much higher over land than over the ocean (Warren et al. 2007).

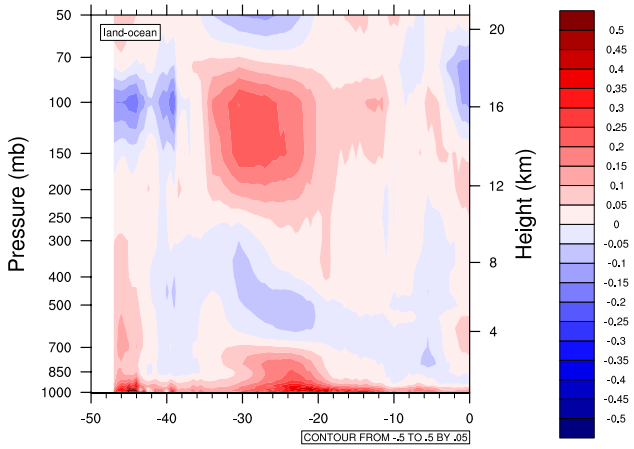

Fig. 7 Differences in mean temperature change profiles (2060–2079 minus 1990–2009) between land and ocean (land–ocean) for the NARCliM ensemble (unit: °C). Here, the changes are not statistically significant

3.3.4 Diurnal variation of changes over land

Future changes in temperature show clear diurnal variation (Fig. 8), especially at levels near the surface (i.e. below 700 hpa). From 12 pm (AEST local time), the near surface layers start to warm faster than layers above, which reach the maximum value at 3 pm, then the warming rate starts to reduce, especially for the tropical region. The faster surface warming will make the near-surface layer become less stable, which can thus provide a suitable environment for convective systems such as storms. In contrast, from 12 a.m. (local time), the near surface layers start to cool faster than the layers above, which reach the maximum cooling rate at 6 a.m., after which the cooling rate starts to reduce. The faster cooling rate for the surface levels than layers above during the early morning can contribute to favourable conditions for temperature inversions.

Other clear diurnal variations are evident for the tropical region where the troposphere warms faster in the afternoon (12–6 p.m.) than during the early morning (12–6 a.m.). This variation is possibly associated with diurnal variation of the amount of cloud cover in the tropical region (Cairns 1995; Stubenrauch et al. 2006).

3.3.5 Differences between simulations

The results presented thus far have been averages over the 12-member NARCliM ensemble, and here we separate the models by their RCM and GCM characteristics. For simplicity, the simulations driven by the same GCM are referred to as "same GCM driven simulations", the simulations using the same RCM are referred to as "same RCM used simulations" (Table 1). In total, there were 4 "same GCM driven simulations" (average of three members) and 3 "same RCM used simulations" (average of four members).

Differences of changes in temperature among "same GCM driven /same RCM used simulations" are presented in Figs. 9 and 10. All "same GCM driven simulations" project similar changes in pattern with the mean changes shown in Fig. 4, however, the change magnitudes are quite different with the largest changes for ECHAM5 driven simulations and the smallest changes for CSIRO-MK3.0 driven simulations. When comparing future changes derived from "same GCM driven simulations (Fig. 9) and their driven GCMs (Figure S4), it is clear that the differences of changes in temperature between "same GCM driven simulations" are largely inherited from the driving GCMs. Changes in temperature projected by the 3 "same RCM used simulations" are similar (Fig. 10). All RCMs project not only a similar pattern in mean changes but also similar magnitude of changes. As there are only 4 and 3 simulations for a "same GCM driven simulation" and "same RCM used simulation", the ensemble size is too small to analyze model significance/agreement as per Fig. 4.

"Same GCM driven/same RCM used simulations" generally show similar patterns for changes in temperature profiles. Larger differences are observed between "same GCM driven simulations" than "same RCM used simulations". This suggests that large-scale GCM inputs driving the RCMs play a critical role in determining changes in atmospheric temperature.

4 Discussion

In this study, we used the NARCliM outputs (dynamically downscaled CMIP3 GCMs) to assess future changes in vertical temperature profiles for the Australasian region (Fig. 4). We also compared the NARCliM simulated future temperature changes at four pressure levels with those derived from the more recent CORDEX simulations (dynamically downscaled CMIP5 GCMs). Mean changes of temperature profiles derived from NARCliM and CORDEX were found to show similar patterns (Fig. 5), even if larger increases in temperature are projected from the CORDEX simulations than NARCliM simulations. These results are consistent with Fig. 12.12 in the IPCC AR5 report (https://www.climatechange2013.org/images/figures/WGI_AR5_Fig12-12.jpg) (Collins et al. 2013), even though both the simulations and reference periods are different between the two studies. The results shown in the IPCC reports are derived from the multiple CMIP5 GCMs for three different RCPs (RCP2.6, RCP4.5 and RCP8.5). The differences are the global zonal mean changes for 2081–2100 relative to 1986–2005. The results in our study are however derived from the dynamical downscaled CMIP3 GCM ensemble for the A2 emission scenario for 2060–2079 relative 1990–2009. In spite of the different time periods and emission scenarios, our results show similar changes as shown in Collins et al. 2013, at least in the change in the spatial pattern of temperature including the increase in temperature for the troposphere, the decrease in temperature for the lower stratosphere, and larger increase in temperature for higher emission scenario. However, the magnitude of change is slightly different, which can be attributed to the different GCMs, emission scenarios, reference periods and the regional models.

Future changes in temperature shown in Fig. 4 will lead to changes in atmospheric stability. Convective available potential energy (CAPE), convective inhibition (CIN), the lifted condensation level (LCL), and the level of free convection (LFC) are all widely used to describe the conditionally unstable processes. CAPE is projected to increase more than CIN, however, LCL and LFC are projected to decrease for Central and Northern Australia, which indicates that the atmosphere will be more conditionally unstable. In contrast,

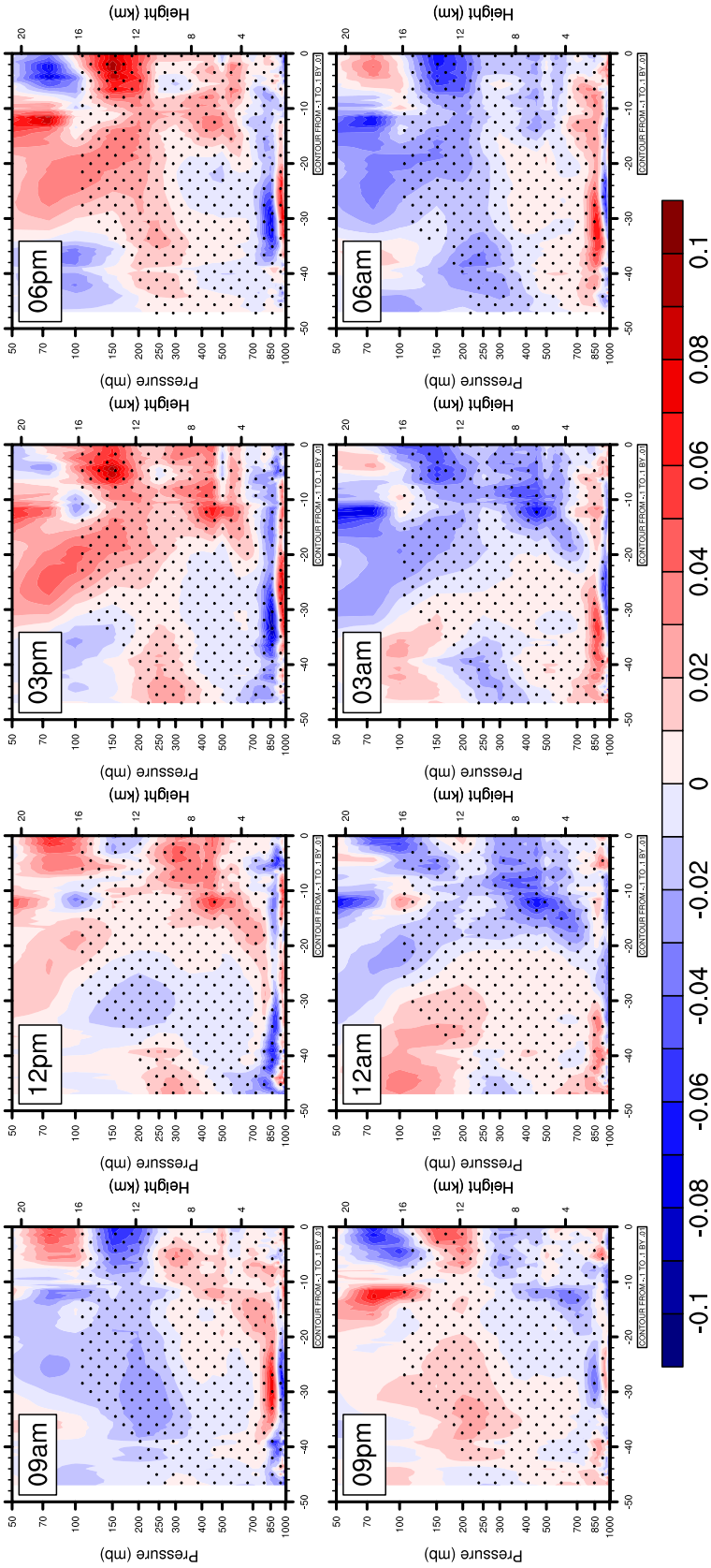

Fig. 8 Diurnal variation of changes in temperature (2060–2079 minus 1990–2009) anomaly (relative to mean changes shown in Fig. 4) over land for the NARCliM ensemble (units: °C). Here the stripling denotes significant change and 80% agreement in the sign of the change between 12 ensemble members

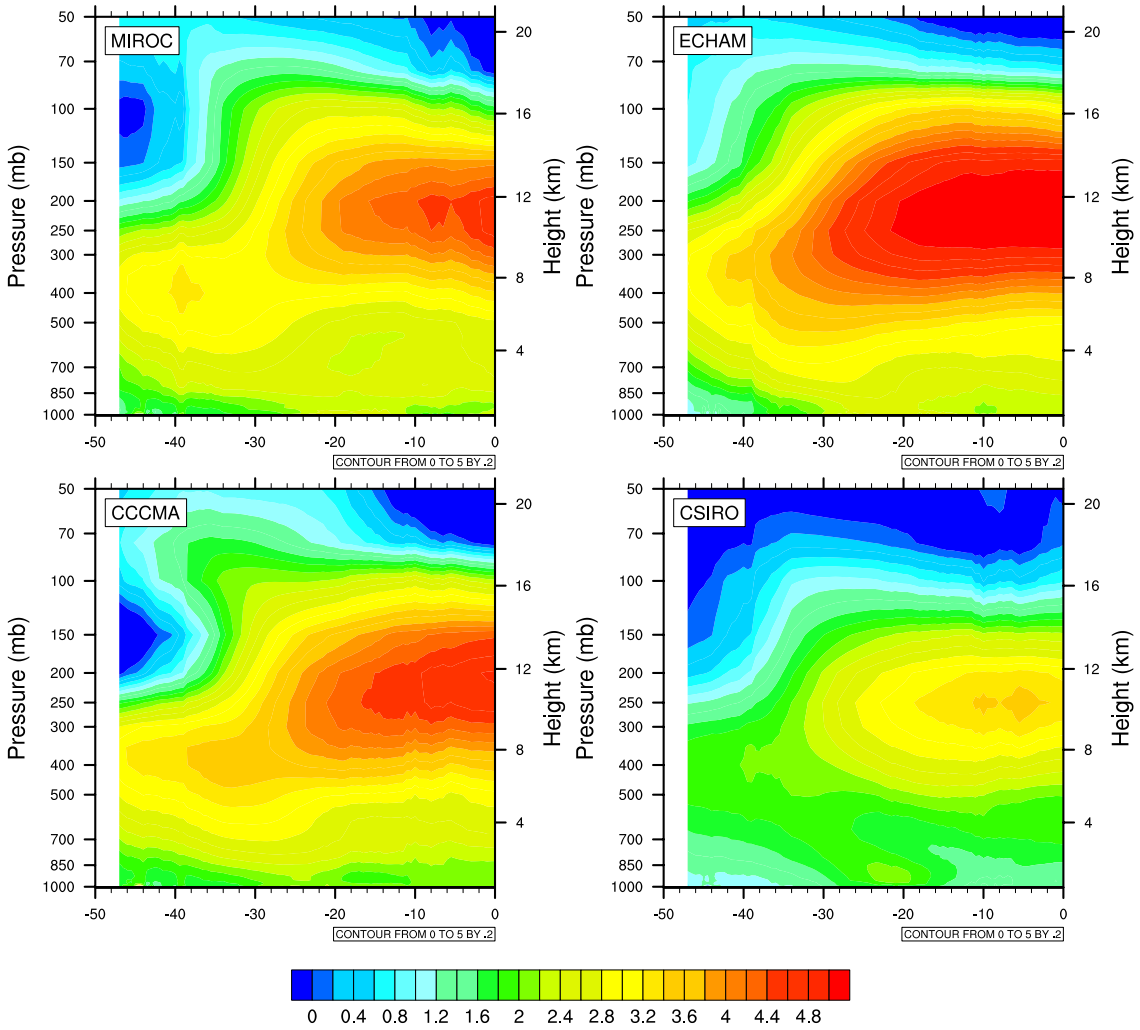

Fig. 9 Changes in temperature (2060–2079 minus 1990–2009) for "same GCM driven simulations" for the NARCliM ensemble (units: ^{o}C)

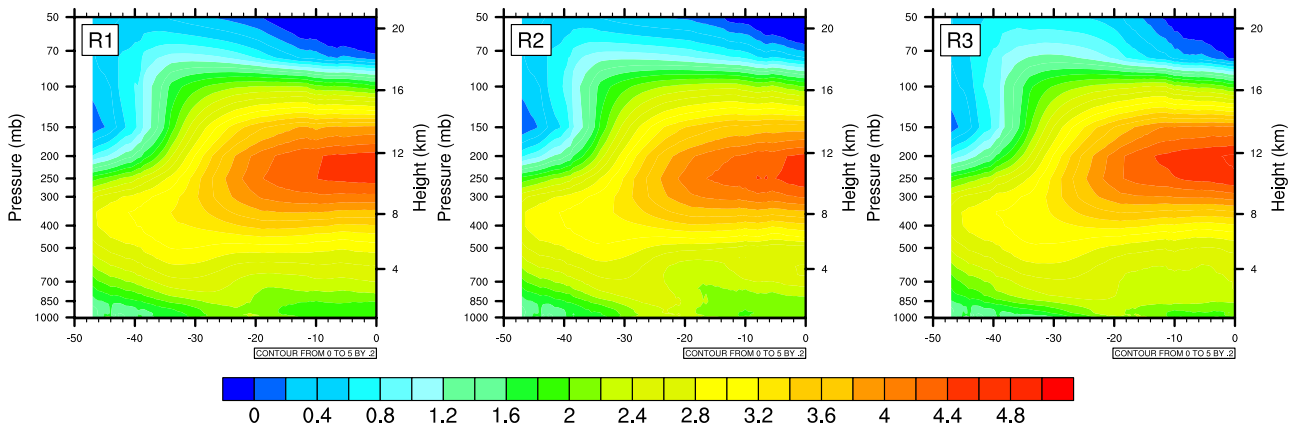

Fig. 10 Changes in temperature (2060–2079 minus 1990–2009) for "same RCM used simulations" for the NARCliM ensemble(units: ^{o}C)

CAPE is projected to increase a little, but CIN, LCL and LFC are projected to increase strongly in Southern Australia, which suggests that the atmosphere will become less conditionally unstable in the future (Figure S5).

Higher temporal resolution (3 hourly) of RCM modelling outputs makes it possible to analyse diurnal variation of future changes in temperature. As shown Fig. 8, the lower troposphere (below 850 hPa) is found to be less stable in the afternoon and more stable in the early morning. These changes will directly impact on a variety of weather systems. For instance, in Australia, thunderstorms mostly occur in the afternoon and peak around 6 p.m. local time (Allen et al. 2011). The lower troposphere is projected to be less stable in the late afternoon, which will potentially increase the occurrence of thunderstorms. More work is required to analyse thunderstorm and severe thunderstorm related indices for assessing the impact of temperature profile changes on the frequency and intensity of thunderstorm events. Temperature inversions (i.e. near surface inversions) mostly occur in the early morning (Ji et al. 2018). The lower troposphere is projected to be more stable in the early morning, which indicated an increased possibility for temperature inversions in the future. Ji et al. (2018) analysed future changes in near surface temperature inversions for southeast Australia (the 10 km NARCliM domain shown in the red box in Fig. 1) and concluded that more near surface inversions with longer duration will occur over the southern land areas, and fewer inversions with shorter duration will occur over the northern land areas, but their strength increases everywhere. These seem to conflict with the conclusions of this study. However, changes in temperature at near surface level (Fig. 8) do show faster increases in temperature at surface levels as compared to the layers above for areas north of 30° S, which supports the conclusion in Ji et al. (2018). The results in this study also indicated more suitable conditions for temperature inversions in the early morning but not necessarily near surface inversions.

As dynamical downscaling takes substantial time to create regional climate simulations, relatively old CMIP3 GCM downscaled simulations and available CMIP5 GCM downscaled simulations were used in this study. They indicated similar changes in the spatial pattern (Fig. 5), however, the uncertainties between NARCliM/CORDEX simulations are relatively large (not shown), but it is reflected in the differences between different GCM driven simulations (Fig. 9). When more CMIP5 GCMs downscaled simulations and new CMIP6 GCMs downscaled simulations become available the projected changes in atmospheric temperature should be reviewed.

From the results for "same GCM driven simulations" and "same RCM used simulations", it can be seen that changes in temperature between "same RCM used simulations" are similar. In contrast, those between "same GCM driven simulations" are quite different in magnitude (Fig. 9). This is understandable, as the GCMs selected in the NARCliM project were chosen based on a number of criteria that include spanning the range of future changes across the CMIP3 GCMs (Evans et al. 2014). For Australia, MIROC3.2 projects a slightly warmer and much wetter future, CCCMA3.1 projects a hotter and slightly wetter future, CSIRO-MK3.0 projects a slightly warmer and drier future, and ECHAM5 projects a hotter and slightly drier future. The differences in temperature and humidity projected by the four GCMs result in diverse changes in temperature magnitude for the four "same GCM used simulations" (Fig. 9). This is consistent with findings from previous uncertainty studies, which suggest that the largest uncertainty in future projections is sourced from GCMs (Teng et al. 2012). These imply that careful selection of GCMs is required to capture the range of future changes within the full GCM ensemble when performing dynamical downscaling projects.

5 Summary and conclusions

The main objective of this study is to assess how atmospheric vertical temperature profiles might change under future climate conditions using an ensemble of regional climate model simulations. We first analyzed temperature trends in observed records and in four reanalysis datasets, then we focused on far future changes of mean temperature relative to the historical period, including seasonal and diurnal variations, and differences between members of the ensemble.

Trends in observations and the four reanalysis datasets show faster warming in the troposphere than the surface, and cooling in the lower stratosphere. These temperature trends are projected to continue with accelerated warming rate in the future. These changes in temperature are found to be latitude-dependent, with much larger increases in the tropical regions as compared to the temperate region, particularly for the upper troposphere levels i.e. between 200 and 300 hPa.

The results show that air temperature warms more over land than over oceans in the lower troposphere, and less over land than over oceans for the middle troposphere, which indicates that the atmosphere in the lower troposphere over land will be less stable than that over ocean, especially in summer.

The results also show clear seasonal and diurnal variations in temperature changes. Temperature generally increases faster in summer than in winter, especially for higher latitude areas. Diurnal variation of changes indicates that the lower troposphere will be less stable in the afternoon and more stable in the early morning, which will directly

impact weather systems such as thunderstorms and temperature inversions.

Uncertainties between simulations are found to be relatively large, especially when considering RCM simulations driven by different GCMs. This suggests that careful selection of GCMs, including consideration of the range of future changes present in the GCM ensemble, is required when dynamically downscaling projections in order to adequately sample this future change uncertainty.

In conclusion, the results of this study indicate that the rate of vertical temperature changes will increase in the troposphere in the future, with clear regional, seasonal and diurnal variations. These results have important consequences for projections of some extreme weather phenomena which should be further investigated in future work.

Acknowledgements This work is made possible by funding from the NSW Environmental Trust for NSW/ACT Regional Climate Modelling Project (NARCliM), and the Australian Research Council as part of the Future Fellowship FT110100576 and Linkage Project LP120200777. A. Di Luca was supported by the Australian Research Council grants DE170101191. The modelling work was undertaken on the NCI high performance computers in Canberra, Australia, which is supported by the Australian Commonwealth Government.

We would like to thank Branislava Jovanovic at Australian Bureau of Meteorology for providing the homogenized monthly upper-air temperature dataset for Australia. This made it possible to investigate observed changes in temperature profile for Australia.

References

Aikawa M, Hiraki T (2009) Characteristic seasonal variation of vertical air temperature profile in urban areas of Japan. Meteorol Atmos Phys 104:95–102

Aires F, Prigent C, Orlandi E, Milz M, Eriksson P, Crewell S, Lin CC, Kangas V (2015) Microwave hyperspectral measurements for temperature and humidity atmospheric profiling from satellite: the clear-sky case. J Geophys Res-Atmos 120:11334–11351

Allen JT, Karoly DJ, Mills GA (2011) A severe thunderstorm climatology for Australia and associated thunderstorm environments. Aust Meteorol Oceanogr J 61(3):143–158

Blumberg WG, Turner DD, Lohnert U, Castleberry S (2015) Ground-based temperature and humidity profiling using spectral infrared and microwave observations. Part II: actual retrieval performance in clear-sky and cloudy conditions. J Appl Meteorol Climatol 54:2305–2319

Bourne SM, Bhatt US, Zhang J, Thoman R (2010) Surface-based temperature inversions in Alaska from a climate perspective. Atmos Res 95:353–366

Byrne MP, O'Gorman PA (2013) Land-Ocean warming contrast over a wide range of climates: convective quasi-equilibrium theory and idealized simulations. J Clim 26:4000–4016

Cairns B (1995) Diurnal variations of cloud from ISCCP data. Atmos Res 37:133–146

Chahine MT, Coauthors (2006) AIRS improving weather forecasting and providing new data on greenhouse gases. BAMS 87:910–926

Chikira M, Sugiyama M (2010) A cumulus parameterization with state-dependent entrainment rate. Part I: description and sensitivity to temperature and humidity profiles. J Atmos Sci 67:2171–2193

Christy JR, Norris WB (2006) Satellite and VIZ-radiosonde intercomparisons for diagnosis of nonclimatic influences. J Atmos Oceanic Technol 23:1181–1194

Christy JR, Norris WB (2009) Discontinuity issues with radiosonde and satellite temperatures in the Australian Region 1979–2006. J Atmos Oceanic Technol 26:508–522

Christy JR, Norris WB, Redmond K, Gallo KP (2006) Methodology and results of calculating central california surface temperature trends: evidence of human-induced climate change? J Clim 19:548–563

Christy JR, Norris WB, McNider RT (2009) Surface temperature variations in East Africa and possible causes. J Clim 22:3342–3356

Christy JR, Spencer RW, Norris WB (2011) The role of remote sensing in monitoring global bulk tropospheric temperatures. Int J Remote Sens 32:671–685

Clarke H, Evans JP (2019) Exploring the future change space for fire weather in southeast Australia. Theoret Appl Climatol 136:513–527. https://doi.org/10.1007/s00704-018-2507-4

Bony S, Coauthors (2006) How well do we understand and evaluate climate change feedback processes? J Clim 19:3445–3482

Collins M, Knutti R, Arblaster J, Dufresne J-L, Fichefet T, Friedlingstein P, Gao X, Gutowski WJ, Johns T, Krinner G, Shongwe M, Tebaldi C, Weaver AJ and Wehner M (2013) Long-term Climate Change: Projections, Commitments and Irreversibility. In: Stocker TF, Qin D, Plattner G-K, Tignor M, Allen SK, Boschung J, Nauels A, Xia Y, Bex V and Midgley PM (eds) Climate Change 2013: the physical science basis. contribution of working group I to the fifth assessment report of the intergovernmental panel on climate change. Cambridge University Press, Cambridge, United Kingdom and New York, NY, USA.

Cortés-Hernández VE, Zheng F, Evans J et al (2015) Evaluating regional climate models for simulating sub-daily rainfall extremes. Clim Dyn 47:1613–1628. https://doi.org/10.1007/s00382-015-2923-4

Dee DP, Uppala SM, Simmons AJ, Berrisford P, Poli P, Kobayashi S, Andrae U, Balmaseda MA, Balsamo G, Bauer P, Bechtold P, Beljaars ACM, van de Berg L, Bidlot J, Bormann N, Delsol C, Dragani R, Fuentes M, Geer AJ, Haimberger L, Healy SB, Hersbach H, Hólm EV, Isaksen L, Kållberg P, Köhler M, Matricardi M, McNally AP, Monge-Sanz BM, Morcrette J-J, Park B-K, Peubey C, de Rosnay P, Tavolato C, Thépaut J-N, Vitart F (2011) The ERA-Interim reanalysis: configuration and performance of the data assimilation system. Q J Roy Meteorol Soc 137:553–597

Di Luca A, de Elía R, Laprise R (2013) Potential for small scale added value of RCM's downscaled climate change signal. Clim Dyn 40:601–618

Di Luca A, Evans JP, Pepler A et al (2016a) Australian east coast lows in a regional climate model ensemble. J Southern Hemisphere Earth Syst Sci 66:108–124

Di Luca A, Argüeso D, Evans JP, de Elía R, Laprise R (2016b) Quantifying the overall added value of dynamical downscaling and the contribution from different spatial scales. J Geophys Res 121:1575–1590

Di Virgilio G, Evans JP, Blake SAP et al (2019a) Climate change increases the potential for extreme wildfires. Geophys Res Lett 46:8517–8526. https://doi.org/10.1029/2019GL083699

Di Virgilio G, Evans JP, Di Luca A, Olson R, Argueso D, Kala J, Andrys J, Hoffmann P, Katzfey JJ, Rockel B (2019b) Evaluating reanalysis-driven CORDEX regional climate models over Australia: model performance and errors. Clim Dyn 53:2985–3005

Di Virgilio G, Evans JP, Di Luca A et al (2020) Realised added value in dynamical downscaling of Australian climate change. Clim Dyn 54:4675–4692. https://doi.org/10.1007/s00382-020-05250-1

Evans JP, Ekström M, Ji F (2012) Evaluating the performance of a WRF physics ensemble over South-East Australia. Clim Dyn 39:1241–1258

Evans JP, Fita L, Argüeso D and Liu Y (2013a) Initial NARCliM evaluation. In: Piantadosi J, Anderssen RS, Boland J (eds) MODSIM2013, 20th International Congress on Modelling and Simulation. Modelling and Simulation Society of Australia and New Zealand, December 2013, pp 2765–2771

Evans JP, Ji F, Abramowitz G, Ekström M (2013) Optimally choosing small ensemble members to produce robust climate simulations. Environ Res Lett 8:044050

Evans JP, Ji F, Lee C, Smith P, Argüeso D, Fita L (2014) Design of a regional climate modelling projection ensemble experiment—NARCliM. Geosci Model Dev 7:621–629

Evans JP, Argueso D, Olson R, Di Luca A (2017) Bias-corrected regional climate projections of extreme rainfall in south-east Australia. Theoret Appl Climatol 130:1085–1098

Evans JP, Kay M, Prasad A, Pitman A (2018) The resilience of Australian wind energy to climate change. Environ Res Lett 13:024014. https://doi.org/10.1088/1748-9326/aaa632

Fita L, Evans JP, Argüeso D et al (2016) Evaluation of the regional climate response in Australia to large-scale climate modes in the historical NARCliM simulations. Clim Dyn. https://doi.org/10.1007/s00382-016-3484-x

Giorgi F, Jones C, Asrar G (2009) Addressing climate information needs at the regional level: the CORDEX framework. WMO Bull 53:175–183

Grise KM, Thompson DW (2012) Equatorial planetary waves and their signature in atmospheric variability. Je Atmos Sci 69:857–874. https://doi.org/10.1175/JAS-D-11-0123.1

Hartmann DL, Klein Tank AMG, Rusticucci M, Alexander LV, Bronnimann S, Charabi Y, Dentener FJ, Dlugokencky EJ, Easterling DR, Kaplan A, Soden BJ, Thorne PW, Wild M and Zhai PM (2013) Observations: atmosphere and surface. In: Stocker TF, Qin D, Plattner G-K, Tignor M, Allen SK, Boschung J, Nauels A, Xia Y, Bex V and Midgley PM (eds) Climate change 2013: the physical science basis. Contribution of working group I to the fifth assessment report of the intergovernmental panel on climate change. Cambridge University Press, Cambridge, United Kingdom and New York, NY, USA

Ji F, Ekström M, Evans JP, Teng J (2014) Evaluating rainfall patterns using physics scheme ensembles from a regional atmospheric model. Theoret Appl Climatol 115:297–304

Ji F, Evans JP, Teng J, Scorgie Y, Argüeso D, Di Luca A (2016) Evaluation of long-term precipitation and temperature Weather Research and Forecasting simulations for southeast Australia. Climate Res 67:99–115

Ji F, Evans JP, Di Luca A, Jiang NB, Olson R, Fita L, Argueso D, Chang LT-C, Scorgie Y, Riley M (2018) Projected change in characteristics of near surface temperature inversions for Southeast Australia. Clim Dyn 52(3):1487–1503

Jones TA, Stensrud DJ (2012) Assimilating AIRS temperature and mixing ratio profiles using an ensemble Kalman filter approach for convective-scale forecasts. Weather Forecast 27:541–564

Jovanovic B, Smalley R, Timbal B, Siems S (2016) Homogenized monthly upper-air temperature data set for Australia. Int J Climatol 37:3209–3222

Jovanovic B, Smalley R, Timbal B, Siems S (2016) Homogenized monthly upper-air temperature data set for Australia. Int JClimatol 37:3209-3222

Kalnay E, Kanamitsu M, Kistler R et al (1996) The NCEP/NCAR 40-year reanalysis project. Bull Am Meteor Soc 77:437–470

Kobayashi S, Ota Y, Harada Y, Ebita A, Moriya M, Onoda H, Onogi K, Kamahori H, Kobayashi C, Endo H, Miyaoka K, Takahashi K (2015) The JRA-55 reanalysis: general specifications and basic characteristics. J Meteorol Soc Jpn Ser II 93:5–48

Ma XL, He J, Ge XY (2017) Simulated sensitivity of the tropical cyclone eyewall replacement cycle to the ambient temperature profile. Adv Atmos Sci 34:1047–1056

McGregor JL, Nguyen KC, Kirono DGC, Katzfey JJ (2016) High resolution climate projections for the islands of Lombok and Sumbawa, Nusa Tenggara Barat Province, Indonesia: Challenges and implications. Clim Risk Manag 12:32–44

Mears CA, Wentz FJ, Thorne PW (2012) Assessing the value of Microwave Sounding Unit-radiosonde comparisons in ascertaining errors in climate data records of tropospheric temperatures. J Geophys Res 117:D19103

Newsom RK, Turner DD, Goldsmith JEM (2013) Long-term evaluation of temperature profiles measured by an operational Raman lidar. J Atmosp Oceanic Technol 30:1616–1634

Olson R, Evans J, Di Luca A, Argueso D (2016) The NARCliM project: Model agreement and significance of climate projections. Clim Res 69:209–227

Po-Chedley S, Fu Q (2012) A bias in the Midtropospheric Channel Warm Target Factor on the NOAA-9 microwave sounding unit. J Atmos Oceanic Technol 29:646–652

Pralungo LR, Haimberger L (2015) New estimates of tropical mean temperature trend profiles from zonal mean historical radiosonde and pilot balloon wind shear observations. J Geophys Res-Atmos 120:3700–3713

Raju A, Parekh A, Chowdary JS, Gnanaseelan C (2014) Impact of satellite-retrieved atmospheric temperature profiles assimilation on Asian summer monsoon 2010 simulation. Theoret Appl Climatol 116:317–326

Ramaswamy V, Schwarzkopf MD (2002) Effects of ozone and well-mixed gases on annual mean stratospheric temperature trends. Geophys Res Lett 29(22):2064

Ramaswamy V, Schwarzkopf MD, Randel WJ, Santer BD, Soden BJ, Stenchikov GL (2006) Anthropogenic and natural influences in the evolution of lower stratospheric cooling. Science 311:1138–1141

Randall RM, Herman BM (2008) Using limited time period trends as a means to determine attribution of discrepancies in microwave sounding unit-derived tropospheric temperature time series. J Geophys Res 113:D05105

Rieckh T, Scherllin-Pirscher B, Ladstädter F, Foelsche U (2014) Characteristics of tropopause parameters as observed with GPS radio occultation. Atmos Meas Tech 7:3947–3958

Rienecker MM, Suarez MJ, Gelaro R, Todling R, Bacmeister J, Liu E, Bosilovich MG, Schubert SD, Takacs L, Kim G-K, Bloom S, Chen J, Collins D, Conaty A, Silva Ad, Gu W, Joiner J, Koster RD, Lucchesi R, Molod A, Owens T, Pawson S, Pegion P, Redder CR, Reichle R, Robertson FR, Ruddick AG, Sienkiewicz M, Woollen J (2011) MERRA: NASA's modern-era retrospective analysis for research and applications. J Clim 24:3624–3648

Santer BD, Penner JE, Thorne PW (2006) How well can the observed vertical temperature changes be reconciled with our understanding of the causes of these changes? In temperature trends in the lower atmosphere: steps for understanding and reconciling differences. In: Karl TR, Hassol SJ, Miller CD and Murray WL (eds) A Report by the Climate Change Science Program and the Subcommittee on Global Change Research, Washington, DC

Skamarock WC, Klemp JB, Dudhia J, Gill DO, Barker DM, Duda MG, Huang XY, Wang W, Powers JG (2008) A description of the advanced research WRF Version 3, NCAR Technical Note. NCAR, Boulder

Stovern DR, Ritchie EA (2016) Simulated sensitivity of tropical cyclone size and structure to the atmospheric temperature profile. J Atmos Sci 73:4553–4571

Stubenrauch CJ, Chedin A, Radel G, Scott NA, Serrar S (2006) Cloud properties and their seasonal and diurnal variability from TOVS path-B. J Clim 19:5531–5553

Tebaldi C, Arblaster JM, Knutti R (2011) Mapping model agreement on future climate projections. Geophys Res Lett 38

Teng J, Vaze J, Chiew FHS, Wang B, Perraud J-M (2012) Estimating the Relative Uncertainties Sourced from GCMs and Hydrological

Models in Modeling Climate Change Impact on Runoff. Journal of Hydrometeorology 13:122–139
Trewin B (2013) A daily homogenized temperature data set for Australia. Int J Climatol 33:1510–1529
Wang KC, Liang SL (2009) Global atmospheric downward longwave radiation over land surface under all-sky conditions from 1973 to 2008. J Geophys Res 114:D19101
Warren SG, Eastman RM, Hahn CJ (2007) A survey of changes in cloud cover and cloud types over land from surface observations, 1971–96. J Clim 20:717–738
Zhang K, Fu E, Silcock D, Wang Y, Kuleshov Y (2011) An investigation of atmospheric temperature profiles in the Australian region using collocated GPS radio occultation and radiosonde data. Atmos Measur Tech 4:2087–2092
Zhang K, Wu CQ, Li J (2016) Retrieval of atmospheric temperature and moisture vertical profiles from satellite advanced infrared sounder radiances with a new regularization parameter selecting method. J Meteorol Res 30:356–370
Zheng J, Li J, Schmit TJ, Li JL, Liu ZQ (2015) The impact of AIRS atmospheric temperature and moisture profiles on hurricane forecasts: Ike (2008) and Irene (2011). Adv Atmos Sci 32:319–335
Ziarani MR, Bookhagen B, Schmidt T, Wickert J, de la Torre A, Hierro R (2019) Using convective available potential energy (CAPE) and dew-point temperature to characterize rainfall-extreme events in the south-central Andes. Atmosphere 10:379